International Journal of Engineering Research & Technology (IJERT)
ISSN: 2278-0181
Vol. 15 Issue 09 , September - 2026

Performance Evaluation of a Fluid-Based Beam Splitting Photovoltaic-Thermal System Using TiO2 Nanofluid Spectral Filter

Pushparaj Jiwanapurkar[1], Hitesh Bhargav[2,*]

[1]Research Scholar, Mechanical Engineering, Gujarat Technological University, Ahmedabad, Gujarat, India

[2]Asst. Professor, Dept. of Mechanical Engineering, BVM Engineering College, Vallabh Vidyanagar-388120, Gujarat, India

Abstract **-** This study presents the design, fabrication, and outdoor performance evaluation of a fluid-based spectral beam-splitting photovoltaic-thermal (BSPVT) system employing a TiO2 nanofluid (0.04% w/w) as an optical filtering medium. A modular experimental rig consisting of a PMMA fluid filter, hinged MS frame, and controlled circulation system is used to simultaneously monitor electrical and thermal performance of the system under natural sunlight. The TiO2 nanofluid demonstrated strong absorption of thermal wavelengths while maintaining adequate transmissivity in the c-Si responsive region, thereby reducing PV thermal loading and enhancing total energy utilization. Outdoor experiments conducted in Daman showed that the nanofluid filter reduced PV temperature by 12-15 degC, stabilizing mid-day electrical efficiency at ~7.4-9.4% compared with 6-8% for the unfiltered module. Thermal efficiency ranged from 45-80% depending on flow rate, contributing to peak overall efficiencies of 68% (50 LPH), 73% (60 LPH), and 85% (70 LPH). Although slight optical attenuation caused minor early-hour electrical loss, this was offset by substantial thermal gains. The results establish feasibility of TiO2 as a low-cost, stable, and highly effective spectral filter for BSPVT applications.

Keywords **-** Spectral beam-splitting; photovoltaic-thermal (PV/T); TiO2 nanofluid; hybrid solar system; experimental setup; thermal efficiency; electrical efficiency; outdoor testing

NOMENCLATURE

BSPVT Beam-Splitting Photovoltaic Thermal
PV Photovoltaic
PVT Photovoltaic Thermal
IR Infrared
NIR Near-Infrared
UV Ultraviolet
TiO2 Titanium Dioxide
MS Mild Steel
PMMA Polymethyl Methacrylate
LPH Litres per Hour (flow rate)

SYMBOLS

Afilter Area of the fluid filter (m2)
Apv Area of the photovoltaic module (m2)
Cp Specific heat capacity of the working fluid (J/kg.K)
Iabove Solar insolation measured above the filter (W/m2)
Ibelow Solar insolation measured below the filter (W/m2)
mf (dot) Mass flow rate of the working fluid (kg/s)
Pmax Maximum electrical power output of PV module (W)
Q Useful heat gained by the working fluid (W)
Tamb Ambient temperature (degC)
Tin Inlet fluid temperature (degC)
Tout Outlet fluid temperature (degC)
Tpv PV temperature (degC)
t Time duration for fluid collection (s)
Vf Volume of fluid collected (m3)
rho_f Density of the working fluid (kg/m3)
beta Tilt angle of the PV-filter assembly (degrees)
eta_th Thermal efficiency of the BSPVT system (%)
eta_ele Electrical efficiency of the PV module (%)
eta_overall Overall efficiency of the BSPVT system (%)

I. INTRODUCTION

The global transition toward low-carbon energy systems has accelerated the deployment of solar-based technologies. While photovoltaic (PV) systems are widely adopted, their effective utilization of the solar spectrum is constrained by the spectral response characteristics of semiconductor materials. Silicon PV cells convert only a limited portion of the incident spectrum region into electricity, while a significant fraction of non-responsive radiation is absorbed as heat [1]. This parasitic heating elevates PV operating temperature, reducing electrical efficiency due to the negative temperature coefficient of silicon and accelerating long-term material degradation [2], [3], [4].

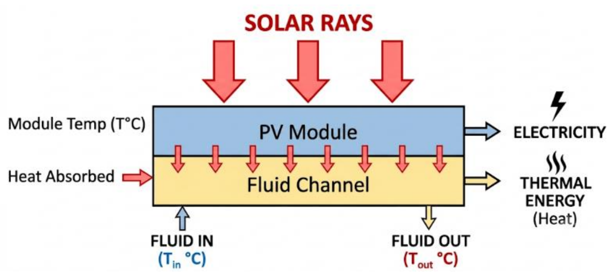

Fig. 1. Conventional PVT system (direct heat absorption).

International Journal of Engineering Research & Technology (IJERT)
ISSN: 2278-0181
Vol. 15 Issue 09 , September - 2026

To address these constraints, hybrid photovoltaic/thermal (PV/T) systems have been developed to recover the excess thermal energy that conventional PV modules dissipate as waste heat. Joshi [5] provides a comprehensive classification of PV/T configurations, in which a conventional arrangement, as illustrated in Fig. 1, places the heat-transfer fluid in direct thermal contact with the back surface of the PV module. While this configuration enables simultaneous electrical and thermal energy production, it also imposes a fundamental performance trade-off between electrical and thermal efficiency because maintaining a low PV temperature is essential for preserving electrical efficiency, but lower temperature limits the attainable thermal output of the system.

Recent developments in PV and PVT cooling emphasize direct absorption and advanced thermal management. Studies show that combining fluids like water [6], air [7], [8], thermic nanofluids [9], [10], PCM [11], etc. with engineered cooling designs including heat sinks and perforated V-shaped fins [7], [10], [12], innovative water channels [13], [14], and hybrid ground heat exchangers [15] substantially lowers PV operating temperatures and boosts overall efficiency. Cooling of the PV by using thermoelectric modules was also attempted [16]. Numerical, experimental, and machine-learning analyses consistently confirm that these approaches improve heat dissipation, stabilize power output, and elevate system performance under real-world conditions [17], [18], [19].

However, because these direct absorption strategies focus primarily on conductive and convective cooling rather than spectral separation, they face a fundamental trade-off: keeping the PV module cool to preserve electrical efficiency inherently restricts the fluid's outlet temperature and limits total thermal yield. This limitation highlights fluid-based spectral beam-splitting as a key complementary strategy for next-generation PVT systems [20].

II. SPECTRAL BEAM SPLITTING

A promising advancement in PV/T design is the incorporation of spectral beam-splitting (SBS) techniques [21]. As illustrated in Fig. 2, the solar spectrum incident on the Earth's surface (300-2500 nm) comprises ultraviolet (UV), visible, and near-infrared (NIR) regions [22], [23], of which only a limited portion lies within the spectral response range of a silicon photovoltaic module [1]. In a beam-split PV/T system, this useful portion of the spectrum is selectively transmitted to the PV receiver for electrical conversion, while the remaining thermally dominant NIR wavelengths are directed toward a separate thermal receiver. This spectral division allows simultaneous harvesting of electrical and thermal energy from the same incident solar flux. By routing the non-useful thermal components away from the PV surface and toward a dedicated absorber, the system enhances PV electrical performance while enabling efficient recovery of thermal energy, thereby improving overall solar utilization.

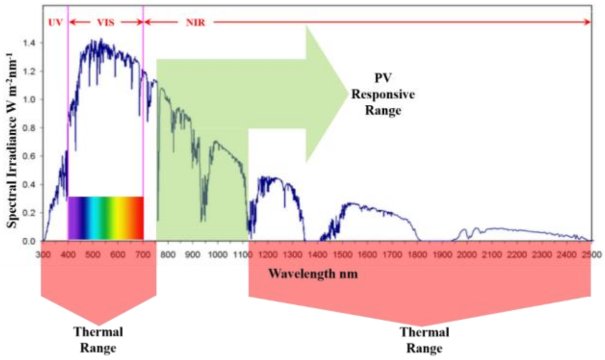

Fig. 2. Spectral irradiance distribution of solar radiation based on the ASTM reference spectrum, illustrating the PV-responsive range and the thermal (non-PV-responsive) range.

Silicon (Si) solar cells exhibit an effective spectral response primarily within the wavelength range of approximately 751-1126 nm [1]. Photons within this band possess sufficient energy to generate electron-hole pairs and thereby contribute directly to electrical power generation. In contrast, photons with wavelengths shorter than 751 nm or longer than 1126 nm are largely ineffective for photovoltaic conversion and instead contribute to parasitic heating of the cell. This defined responsive range is a critical parameter in the design of SBS systems, as it guides the selection of optical filters and working fluids that selectively transmit the useful portion of the spectrum while absorbing or redirecting the non-useful thermal components.

In this approach, an optical filter is positioned above the PV module to selectively transmit the responsive portion of the solar spectrum corresponding to the PV cell's bandgap, while absorbing or redirecting non-responsive wavelengths for thermal harvesting. By more effectively matching the transmitted spectrum to the PV absorption characteristics, SBS systems improve electrical performance while simultaneously enabling efficient utilization of the absorbed thermal energy [24].

Unlike conventional solid-state optical filters, fluid-based spectral filters provide a low-cost, scalable, and highly tunable alternative for spectral management in photovoltaic-thermal applications. These fluids can be engineered or doped with selective nanoparticles, dyes, or absorptive additives to target specific wavelength bands for absorption or transmission, thereby enabling customizable spectral filtering characteristics. In addition to their optical functionality, fluid-based filters inherently offer passive cooling by absorbing infrared radiation and dissipating the

International Journal of Engineering Research & Technology (IJERT)
ISSN: 2278-0181
Vol. 15 Issue 09 , September - 2026

associated thermal load, thereby reducing the operating temperature of the PV module under direct sunlight. A conceptual representation of fluid-based spectral beam splitting is presented in Fig. 3 [25].

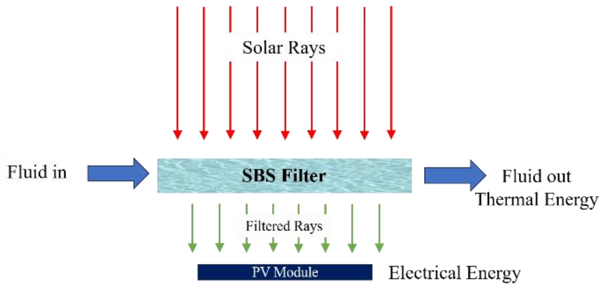

Fig. 3. Conceptual visualization of fluid-based spectral beam splitting [5].

A considerable number of studies have been carried out to identify suitable working fluids whose optical characteristics align with the spectral response of silicon photovoltaic modules. A recent review by Jiwanapurkar et al. [20] provides a detailed assessment of various fluids investigated for SBS applications in PV/T systems. Notably, the majority of these investigations have been conducted under controlled laboratory conditions using solar simulators and typically over short experimental durations. Consequently, the long-term performance, optical stability, and thermal behaviour of these fluids under continuous natural sunlight remain insufficiently explored.

In this context, the present study evaluates the electrical and thermal performance of a fluid-based SBS-PVT system using a modular experimental setup developed by Jiwanapurkar, testing the fluid across various volumetric flow rates.

III. EXPERIMENTAL SETUP

The experimental setup featured in this study, developed by Jiwanapurkar, consists of a custom-designed, cage-type mild steel (MS) frame mounted on a hinged support table, enabling continuous tilt-angle (beta) adjustments via a screw-based inclination mechanism. Situated within the upper portion of the frame is a high-transmissivity PMMA fluid filter (500 x 500 mm with optical path length 10 mm) placed directly above a 10 W silicon PV module. As solar radiation strikes the system, the fluid filter selectively absorbs non-optimal infrared wavelengths into the circulating fluid while transmitting the ideal spectrum to the PV panel below. The closed fluid loop includes a variable-speed pump to control flow rates, along with built-in inlet, outlet, drain, and air-vent ports to ensure stable thermal extraction.

For precise data logging, the system is fully instrumented with K-type thermocouples to record the PV module's back-surface temperature as well as the fluid's inlet and outlet temperatures. Solar irradiance is measured using a pyranometer, allowing direct evaluation of spectral attenuation. Additionally, the electrical parameters including maximum power output (Pmax) under varying load conditions are measured using a solar PV analyser paired with a variable rheostat. Key features of this configuration include modular optical path flexibility, high structural durability for outdoor testing, and decoupled thermal-electrical energy harvesting.

A. Fluid Selection

In a BSPVT system, the absorbing fluid is a critical component that determines both spectral selectivity and thermal energy capture. In this study, a TiO_2 nanofluid with a concentration of 0.04% w/w was selected as the filtering medium. This concentration was identified as optimal based on a prior spectroscopic investigation conducted by Jiwanapurkar [26], which demonstrated that TiO_2 at 0.04% provides an effective balance between strong NIR absorption supporting thermal harvesting and sufficient c-Si responsive range transmission required for efficient photovoltaic conversion.

In the spectroscopic study, Jiwanapurkar [26] analysed twelve nanofluid samples of TiO_2 and ZnO and their combinations (0.01-0.05% w/w) using UV-Vis-NIR spectrophotometry (200-2500 nm). The study confirmed that TiO_2 at 0.04% concentration provides the most effective spectral filtering performance, strongly attenuating non-useful wavelengths while maintaining sufficient transmissivity in the silicon PV response range. This establishes TiO_2 (0.04%) as a suitable nanofluid for enhancing both electrical and thermal performance in BSPVT applications.

The nanofluid was prepared by dispersing TiO_2 nanoparticles in deionized water, followed by ultrasonic agitation to achieve uniform dispersion and minimize agglomeration. A small quantity of sodium dodecyl sulfate (SDS) was added as a surfactant to enhance colloidal stability by reducing surface tension and promoting electrostatic repulsion between particles. This ensured consistent optical behaviour and prevented sedimentation during operation.

IV. METHODOLOGY OF EXPERIMENTATION

The testing process begins by mounting the photovoltaic module within the hinged cage assembly and angling the structure to match the local latitude's optimal tilt angle (beta). To establish a clear performance baseline, the system is first operated in a “no filter” configuration where solar irradiance (I), PV module back-surface temperature (Tpv), ambient temperature (Tamb), and maximum electrical

International Journal of Engineering Research & Technology (IJERT)
ISSN: 2278-0181
Vol. 15 Issue 09 , September - 2026

power output (Pmax) are measured directly under natural sunlight without any optical obstruction.

Next, to isolate the optical transmission losses caused solely by the filter casing, the empty PMMA filter is mounted onto the cage directly above the PV module. During this phase, measurements are recorded for solar insolation both above (Iabove) and below (Ibelow) the filter to evaluate spectral attenuation, alongside continuous logging of Tpv, Tamb, and Pmax.

Finally, the thermal and spectral splitting performance is evaluated by connecting the fluid circulation loop to the filter. The circulating pump is engaged to fill the filter chamber completely with the nanofluid working medium, and the flow control valve is set to the targeted flow rate. In this active operating state, parameters including top and bottom solar insolation (Iabove and Ibelow), fluid inlet and outlet temperatures (Tin and Tout), panel temperature (Tpv), ambient temperature (Tamb), and electrical power generation (Pmax) are simultaneously monitored to assess thermal energy gain and electrical efficiency improvements. Fig. 4 shows a flow chart of the experimental methodology.

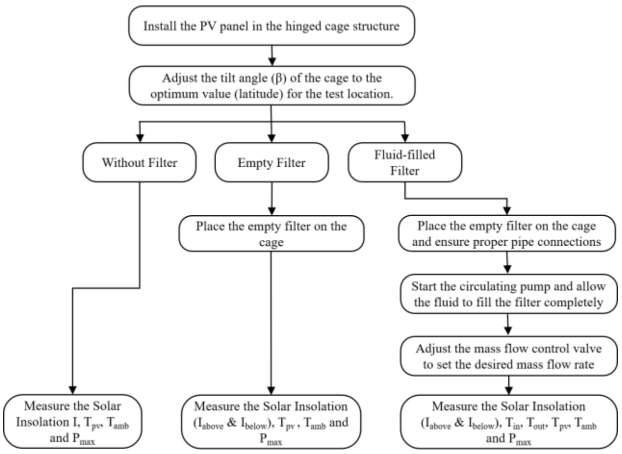

Fig. 4. Experimental procedure flow chart showing the stepwise methodology for performance testing of the BSPVT system under three configurations: no filter, empty filter, and fluid-filled filter.

The comparative performance evaluation follows the sequential testing method established by Jiwanapurkar et al. [27], conducted under real outdoor conditions over five consecutive days. Testing is divided into three distinct operating regimes.

On Day 1, the standalone PV panel is tested without any optical obstruction to establish baseline electrical metrics. On Day 2, the empty PMMA filter casing is placed above the PV module to quantify the optical transmission losses induced by the filter structure itself. From Day 3 to Day 5, the optical filter is filled with a 0.04 wt% TiO2 nanofluid. Operating under steady-state forced circulation, the volumetric flow rate is sequentially adjusted to 50, 60, and 70 LPH on respective days.

During each phase, measurements are logged between 10:00 AM and 5:00 PM for incoming solar irradiance (measured above and below the filter), fluid entry and exit temperatures (Tin and Tout), PV rear surface temperature (Tpv), ambient temperature (Tamb), and electrical power generation (Pmax).

A. Thermal and Electrical Governing Equations

The thermal-electrical characterization and property evaluation follow standard thermodynamic relations and the calculation framework outlined by Joshi et al. [28] and Jiwanapurkar et al. [27]. Specific heat of the nanofluid is calculated using a mass-weighted mixing rule:

$$Cp,nf = (1 - x)Cp,water + xCp,TiO2 \quad (1)$$

where x is the mass fraction of TiO2 nanoparticles in the base fluid. Thermal energy extraction: the useful thermal power collected by the circulating nanofluid, Q, is determined by:

$$Q = m_f \times Cp,nf \times (Tout - Tin) \quad (2)$$

System efficiency metrics: system performance is evaluated through thermal, electrical, and overall efficiency:

$$\eta th = Q / (Iabove \times Afilter),\ \ \eta ele = Pmax / (Iabove \times Apv) \quad (3)$$

$$\eta overall = \eta th + \eta ele \quad (4)$$

V. RESULTS AND DISCUSSION

The experimental performance of the BSPVT system was analyzed for three configurations: (i) no filter (direct sunlight on PV panel); (ii) with empty filter (no fluid in filter chamber); and (iii) with circulating TiO2 nanofluid filter (0.04% w/w concentration) at flow rates of 50, 60, and 70 LPH.

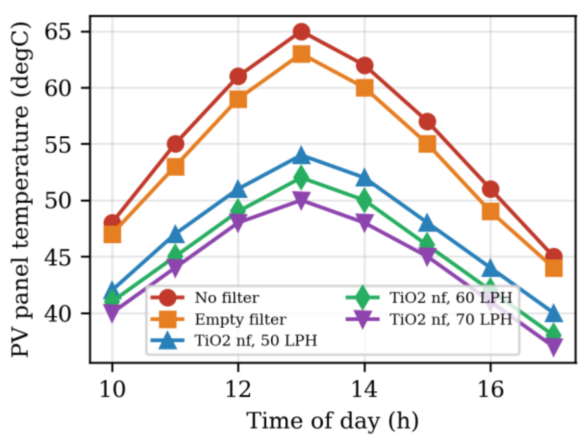

Fig. 5. PV panel temperature variation with time for no filter, empty filter, and TiO2 nanofluid spectral filter at different flow rates (50, 60, and 70 LPH). Reconstructed from values reported in the source manuscript; original data plot not supplied.

International Journal of Engineering Research & Technology (IJERT)
ISSN: 2278-0181
Vol. 15 Issue 09 , September - 2026

Fig. 5 presents the hourly variation in PV panel temperature for the five experimental conditions. The no-filter condition exhibits the highest temperatures throughout the day, with a peak of approximately 65 degC at 13:00. This behavior is expected since the PV panel receives the full solar spectrum, including the thermally dominant NIR portion, resulting in substantial heat accumulation.

The empty filter condition shows a marginal reduction in temperature, approximately 1-2 degC lower than the no-filter case. This minor improvement is attributed to partial shading and the additional optical interface offered by the PMMA enclosure, although no active thermal absorption or cooling takes place.

In contrast, the TiO2 nanofluid filter significantly reduces panel temperature across all flow rates. The cooling effect is most prominent during peak solar hours, where temperatures remain within 50-54 degC, representing a 10-12 degC reduction compared to the no-filter condition. Among the flow conditions, 70 LPH consistently exhibits the lowest temperature profile, indicating that increased flow rate enhances convective heat removal from the filter medium. These results demonstrate the thermal management capability of TiO2 nanofluid, which absorbs NIR radiation and continuously transports the absorbed thermal energy away from the filter through fluid circulation.

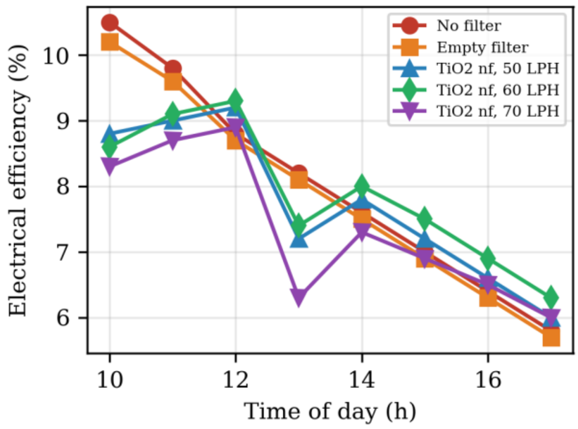

Fig. 6. Variation of electrical efficiency with time for no filter, empty filter, and TiO2 nanofluid spectral filter at different flow rates (50, 60, and 70 LPH). Reconstructed from values reported in the source manuscript; original data plot not supplied.

The electrical efficiency trends shown in Fig. 6 follow the expected inverse correlation with panel temperature. In the no-filter and empty-filter cases, where panel temperatures are highest, electrical efficiency declines markedly from morning values of approximately 10-11% to below 6% by late afternoon. This degradation is consistent with the temperature sensitivity of crystalline silicon photovoltaic modules, where increasing cell temperature reduces open-circuit voltage and negatively impacts conversion efficiency.

The nanofluid-filtered cases display comparatively lower efficiency in the early morning, likely due to mild attenuation of responsive wavelengths by the TiO2 suspension. However, during peak irradiance hours (12:00-15:00), the substantial cooling provided by the nanofluid becomes dominant, resulting in higher efficiencies than both baseline cases. Notably, at 60 LPH and 70 LPH, the system maintains efficiencies between 8-9% during peak conditions, whereas the no-filter and empty-filter cases drop to around 7-8%.

The improved electrical performance under nanofluid operation confirms that spectral beam splitting effectively reduces temperature-induced electrical losses. The results validate the dual benefit of the BSPVT approach: selective transmission of only the useful spectral band for PV conversion, combined with removal of excess thermal load through nanofluid circulation.

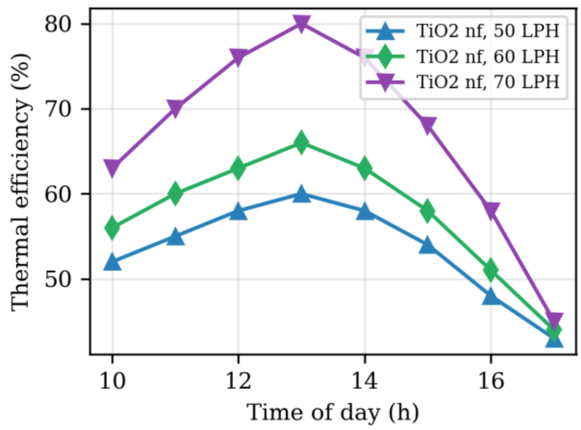

Fig. 7. Variation of thermal efficiency of the TiO2 nanofluid-based BSPVT system at different flow rates (50, 60, and 70 LPH). Reconstructed from values reported in the source manuscript; original data plot not supplied.

Fig. 7 presents the temporal variation of thermal efficiency for the TiO2 nanofluid filter at flow rates of 50, 60, and 70 LPH. Thermal efficiency is reported only for the nanofluid conditions, since the no-filter and empty-filter cases do not incorporate a thermal absorption component. At 10:00, the thermal efficiency begins at approximately 52% for 50 LPH, 56% for 60 LPH, and 63% for 70 LPH, indicating that higher flow rates enhance early-morning heat extraction. As solar irradiance increases, the thermal efficiency rises steadily, reaching mid-day peaks of 60% (50 LPH), 66% (60 LPH), and a significantly higher 80% (70 LPH) at 13:00. This clear performance hierarchy shows that a higher flow rate improves convective heat transport in the fluid, preventing stagnation and enabling continuous absorption of non-responsive radiation. After 15:00, thermal

International Journal of Engineering Research & Technology (IJERT)
ISSN: 2278-0181
Vol. 15 Issue 09 , September - 2026

efficiency declines across all cases due to decreasing solar insolation, falling to 42-45% by 17:00.

Furthermore, the enhanced thermal management provided by the nanofluid also explains the improved electrical efficiency trends observed earlier. For instance, at 13:00, while the no-filter case exhibited an electrical efficiency of only ~8.2% due to elevated panel temperature, the nanofluid cases maintained efficiencies of ~7.2% (50 LPH), ~7.4% (60 LPH), and ~6.3% (70 LPH). Although a slight reduction in electrical output occurs at higher flow rates because of mild optical attenuation, this loss is effectively compensated by the substantial increase in thermal energy recovery, with thermal efficiencies reaching up to 80% at 70 LPH. The overall system performance therefore improves, as the enhanced thermal output more than offsets the marginal electrical reduction, confirming the advantage of BSPVT systems in maximizing total useful energy under real outdoor conditions.

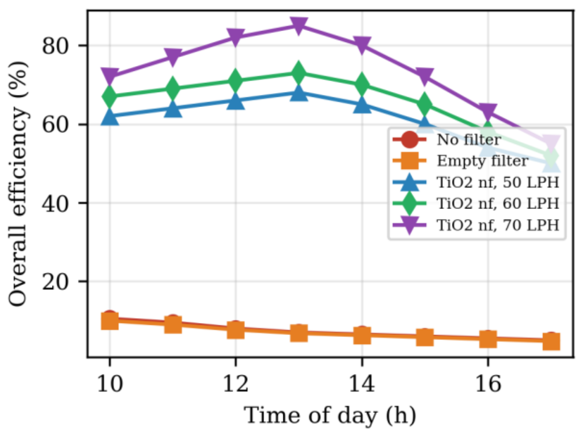

Fig. 8. Variation of overall efficiency of the TiO2 nanofluid-based BSPVT system with time at different flow rates (50, 60, and 70 LPH), compared with electrical efficiency of the no-filter and empty-filter PV configurations. Reconstructed from values reported in the source manuscript; original data plot not supplied.

Fig. 8 illustrates the overall efficiency of the BSPVT system, combining both electrical and thermal outputs for the TiO2 nanofluid filter cases, alongside the purely electrical efficiencies of the no-filter and empty-filter conditions. As expected, the no-filter and empty-filter cases exhibit very low overall efficiencies throughout the day, remaining within 10-11% in the morning and declining to 5-7% by late afternoon, since they contribute only electrical energy and experience significant thermal losses due to high panel temperatures (peaking at 65 degC). In contrast, the nanofluid-enhanced BSPVT system demonstrates substantially higher overall efficiencies due to the combined contribution of thermal energy recovery and reduced PV temperature.

At 10:00, the overall efficiency begins at approximately 62% (50 LPH), 67% (60 LPH), and 72% (70 LPH), indicating that higher flow rates enhance early-morning thermal collection despite similar solar conditions. As solar irradiance increases, the overall efficiency rises sharply, reaching peak values around 13:00 of 68% for 50 LPH, 73% for 60 LPH, and a maximum of ~85% for 70 LPH. These high values correlate strongly with the thermal efficiency trend, where the 70 LPH flow rate likewise peaked at 80% thermal efficiency, driven by enhanced absorption and efficient convective heat removal. The increase in overall efficiency during mid-day is also influenced by the reduction in PV panel temperature observed earlier; the 70 LPH configuration maintained the lowest panel temperature (~50 degC), thereby limiting electrical efficiency degradation during peak heat hours.

After 15:00, overall efficiency declines across all nanofluid cases due to reduced solar availability, falling to 48-52% by 17:00 for the 50 and 60 LPH cases and 55% at 70 LPH. Nevertheless, these values remain significantly higher than the no-filter and empty-filter cases, which drop to 5-6% in the same period. The combined interpretation of all performance indicators, temperature, electrical efficiency, and thermal efficiency, confirms that while the nanofluid filter introduces a slight optical loss, the substantial thermal gain more than compensates for the reduced electrical output. The 70 LPH flow rate offers the best overall system performance by simultaneously lowering PV temperature, maximizing thermal extraction, and thereby delivering the highest overall efficiency throughout the day.

The combined analysis of panel temperature, electrical efficiency, thermal efficiency, and overall efficiency reveals that the volumetric flow rate plays a decisive role in determining the performance of the BSPVT system, with the mid-range flow rate of 60 LPH offering the most favourable balance between electrical and thermal outputs. At higher flow rates (70 LPH), although the system achieves maximum thermal efficiency peaking at ~80% and maintains the lowest PV temperatures (48-52 degC), the increased optical attenuation and rapid heat removal slightly reduce electrical efficiency to ~6.3% at mid-day. Conversely, the lower flow rate of 50 LPH retains better optical transmission but suffers from insufficient cooling, resulting in higher panel temperatures (50-54 degC) and reduced thermal efficiency (60% peak). The 60 LPH condition provides an optimal compromise: it maintains moderate panel temperatures, enabling electrical efficiencies of ~7.4% at peak hours, while concurrently delivering substantial thermal efficiency (~66% at 13:00), leading to stable and high overall efficiency (~73% peak). Thus, the

International Journal of Engineering Research & Technology (IJERT)
ISSN: 2278-0181
Vol. 15 Issue 09 , September - 2026

results clearly indicate that 60 LPH is the optimum flow rate for achieving a balanced enhancement of both electrical and thermal performance in the BSPVT system, ensuring neither component is compromised while maximizing the total useful energy harvested.

VI. CONCLUSION

The present study successfully demonstrated the design, fabrication, and outdoor evaluation of a fluid-based spectral beam-splitting photovoltaic-thermal (BSPVT) system using a low-cost TiO2 nanofluid (0.04% w/w) as the optical filtering medium. The modular experimental rig, featuring a hinged MS frame, interchangeable PMMA filter, and a controlled circulation system, proved capable of reliably capturing the coupled thermal-electrical behaviour of the system under real solar conditions.

Outdoor experimentation showed that the TiO2 nanofluid filter effectively reduced the PV panel temperature by 12-15 degC compared to the no-filter case, lowering peak temperature from 65 degC to 50-53 degC. This temperature reduction directly improved electrical stability, maintaining mid-day electrical efficiencies of 7.4-9.4%, whereas the no-filter configuration declined to 6-8%. The system also demonstrated strong thermal harvesting capability, achieving thermal efficiencies of 60% (50 LPH), ~66% (60 LPH), and up to 80% (70 LPH). Consequently, the combined overall efficiency exceeded 70% for all nanofluid cases, reaching a maximum of ~85% at 70 LPH.

A performance trade-off was observed between electrical and thermal gains: higher flow rates enhanced thermal efficiency but caused slight optical attenuation, reducing electrical output. The 60 LPH condition offered the optimal balance, achieving ~7.4% electrical efficiency, ~66% thermal efficiency, and an overall efficiency of ~73%, making it the most favourable operating point. These results confirm that TiO2 nanofluid can function as a cost-effective spectral filter, offering strong cooling, selective NIR absorption, and robust thermal recovery.

Overall, the study demonstrates that non-plasmonic, easily dispersible TiO2 nanofluid can achieve high outdoor BSPVT performance comparable to or exceeding more expensive nanofluid systems reported in literature. The validated experimental platform provides a strong foundation for extended testing involving year-round performance monitoring, alternative nanofluids, variable path lengths, optical coatings, and degradation studies, supporting further development of scalable and economically viable BSPVT technologies.

B. Recommendations for Future Work

To advance the operational feasibility and thermodynamic performance of fluid-based spectral beam-splitting PVT collectors, future research should focus on multi-scale stability, optical optimization, and rigorous energy accounting. Long-term physical and optical stability analyses of TiO2 nanofluids under prolonged solar exposure are necessary to evaluate surfactant degradation, particle agglomeration, and sedimentation over time. Comparative studies incorporating alternative fluid media such as metal oxides (ZnO, SiO2, CuO) and plasmonic metal nanoparticles (Au/Ag) will establish optimal spectral selectivity across different solar spectrum bands. Varying the fluid filter's optical path length (e.g., 5 mm, 10 mm, and 20 mm) will further reveal the precise trade-off between parasitic optical absorption in the photovoltaic spectrum and thermal absorption gains.

Additionally, conducting year-round outdoor testing across diverse seasonal conditions will capture performance variations driven by changing air mass and solar spectral irradiance. Beyond second-law exergy and comprehensive exergoeconomic assessments to gauge economic viability, practical implementation will require investigating the long-term material degradation of PMMA glazing channels, seals, and adhesives subjected to continuous ultraviolet exposure. Finally, scaling up the fluid channel prototype from lab-scale absorbers to 50-100 W modules will provide crucial insights into flow distribution uniformity, hydraulic pressure drops, and modular integration for commercial rooftop applications.

REFERENCES

[1] R. A. Taylor, T. Otanicar, and G. Rosengarten, "Nanofluid-based optical filter optimization for PV/T systems," Light Sci. Appl., vol. 1, no. 10, pp. e34-e34, 2012, doi: 10.1038/lsa.2012.34.

[2] P. Singh, S. N. Singh, M. Lal, and M. Husain, "Temperature dependence of I-V characteristics and performance parameters of silicon solar cell," Solar Energy Materials and Solar Cells, vol. 92, no. 12, pp. 1611-1616, Dec. 2008, doi: 10.1016/J.SOLMAT.2008.07.010.

[3] D. Tobnaghi, "The Effect of Temperature on Electrical Parameters of Solar Cells," International Journal of Advanced Research in Electrical, Electronics and Instrumentation Engineering, vol. 2, no. 12, pp. 6404-6407, 2013.

[4] A. Kane, V. Verma, and B. Singh, "Optimization of thermoelectric cooling technology for an active cooling of photovoltaic panel," Renewable and Sustainable Energy Reviews, vol. 75, pp. 1295-1305, Aug. 2017, doi: 10.1016/J.RSER.2016.11.114.

[5] S. S. Joshi and A. S. Dhoble, "Photovoltaic-Thermal systems (PVT): Technology review and future trends," Renewable and Sustainable Energy Reviews, vol. 92, pp. 848-882, 2018, doi: 10.1016/j.rser.2018.04.067.

[6] S. S. Joshi and A. S. Dhoble, "Experimental investigation of solar photovoltaic thermal system using water, coconut oil and silicone oil as spectrum filters," Journal of the Brazilian Society of Mechanical

International Journal of Engineering Research & Technology (IJERT)
ISSN: 2278-0181
Vol. 15 Issue 09 , September - 2026

Sciences and Engineering, vol. 39, no. 8, pp. 3227-3236, 2017, doi: 10.1007/s40430-017-0802-0.

[7] W. Fan, G. Kokogiannakis, and Z. Ma, "A multi-objective design optimisation strategy for hybrid photovoltaic thermal collector (PVT)-solar air heater (SAH) systems with fins," Solar Energy, vol. 163, pp. 315-328, Mar. 2018, doi: 10.1016/J.SOLENER.2018.02.014.

[8] M. Tahmasbi, M. Siavashi, A. M. Norouzi, and M. H. Doranehgard, "Thermal and electrical efficiencies enhancement of a solar photovoltaic-thermal/air system (PVT/air) using metal foams," J. Taiwan Inst. Chem. Eng., vol. 124, pp. 276-289, Jul. 2021, doi: 10.1016/J.JTICE.2021.03.045.

[9] N. Karami and M. Rahimi, "Heat transfer enhancement in a PV cell using Boehmite nanofluid," Energy Convers. Manag., vol. 86, pp. 275-285, Oct. 2014, doi: 10.1016/J.ENCONMAN.2014.05.037.

[10] A. N. Al-Shamani, K. Sopian, S. Mat, H. A. Hasan, A. M. Abed, and M. H. Ruslan, "Experimental studies of rectangular tube absorber photovoltaic thermal collector with various types of nanofluids under the tropical climate conditions," Energy Convers. Manag., vol. 124, pp. 528-542, Sep. 2016, doi: 10.1016/J.ENCONMAN.2016.07.052.

[11] M. M. Sarafraz et al., "Experimental investigation on thermal performance of a PV/T-PCM (photovoltaic/thermal) system cooling with a PCM and nanofluid," Energies, vol. 12, no. 13, 2019, doi: 10.3390/en12132572.

[12] S. V. Hudiseanu, F. E. Turcanu, N. C. Cereches, C. G. Popovici, M. Verdes, and I. Huditeanu, "Enhancement of pv panel power production by passive cooling using heat sinks with perforated fins," Applied Sciences, vol. 11, no. 23, Dec. 2021, doi: 10.3390/app112311323.

[13] M. Rosa-Clot, P. Rosa-Clot, and G. M. Tina, "TESPI: Thermal Electric Solar Panel Integration," Solar Energy, vol. 85, no. 10, pp. 2433-2442, 2011, doi: 10.1016/j.solener.2011.07.003.

[14] M. Rosa-Clot, P. Rosa-Clot, G. M. Tina, and C. Ventura, "Experimental photovoltaic-thermal Power Plants based on TESPI panel," Solar Energy, vol. 133, pp. 305-314, 2016, doi: 10.1016/j.solener.2016.03.024.

[15] Y. J. Kim, L. Yang, E. Entchev, S. Cho, E. C. Kang, and E. J. Lee, "Hybrid Solar Geothermal Heat Pump System Model Demonstration Study," Front. Energy Res., vol. 9, Jan. 2022, doi: 10.3389/fenrg.2021.778501.

[16] S. Bulat, E. Buyukbicakci, and M. Erkovan, "Efficiency Enhancement in Photovoltaic-Thermoelectric Hybrid Systems through Cooling Strategies," Energies, vol. 17, no. 2, Jan. 2024, doi: 10.3390/en17020430.

[17] N. Aste, C. Del Pero, and F. Leonforte, "Water PVT Collectors Performance Comparison," Energy Procedia, vol. 105, pp. 961-966, May 2017, doi: 10.1016/J.EGYPRO.2017.03.426.

[18] M. Alobaid, B. Hughes, J. K. Calautit, D. O'Connor, and A. Heyes, "A review of solar driven absorption cooling with photovoltaic thermal systems," Renewable and Sustainable Energy Reviews, vol. 76, pp. 728-742, Sep. 2017, doi: 10.1016/J.RSER.2017.03.081.

[19] S. Tiwari, J. Bhatti, G. N. Tiwari, and I. M. Al-Helal, "Thermal modelling of photovoltaic thermal (PVT) integrated greenhouse system for biogas heating," Solar Energy, vol. 136, pp. 639-649, Oct. 2016, doi: 10.1016/J.SOLENER.2016.07.048.

[20] P. R. Jiwanapurkar, H. A. Bhargav, and B. Ramani, "Fluid based solar spectral beam splitters for hybrid photovoltaic thermal systems: a review," Int. J. Renewable Energy Technology, vol. 14, no. 3, pp. 241-258, 2023.

[21] E. D. Jackson, "Areas for improvement of the semiconductor solar energy converter," in Transactions of the Conference on the Use of Solar Energy, Tucson: Univ. of Arizona Press, 1955, pp. 122-126.

[22] C. S. Solanki, Solar Photovoltaics: Fundamentals, Technologies and Applications, 3rd ed. New Delhi: PHI Learning, 2013.

[23] S. P. Sukhatme and J. K. Nayak, Solar Energy: Principles of Thermal Collection and Storage. Tata McGraw-Hill Education (India), 2015.

[24] A. Mojiri, R. Taylor, E. Thomsen, and G. Rosengarten, "Spectral beam splitting for efficient conversion of solar energy - A review," Renewable and Sustainable Energy Reviews, vol. 28, pp. 654-663, 2013, doi: 10.1016/j.rser.2013.08.026.

[25] R. A. Taylor et al., "Feasibility of nanofluid-based optical filters," Appl. Opt., vol. 52, no. 7, pp. 1413-1422, 2013, doi: 10.1364/AO.52.001413.

[26] P. Jiwanapurkar and H. Bhargav, "Spectroscopic Analysis of Water-Based TiO2 and ZnO Nanofluid for Fluid-Based Beam Split Photovoltaic-thermal System," Journal of Solar Energy Research, vol. 10, pp. 45-55, Mar. 2025, doi: 10.22059/jser.2025.379717.1445.

[27] P. Jiwanapurkar, H. Bhargav, C. Sonawane, C. K. Chan, D. Varsheny, and S. Dixit, "Experimental investigation of a TiO2 nanofluid spectral beam-splitting photovoltaic-thermal system under outdoor conditions," Discover Nano, vol. 21, no. 1, p. 94, 2026, doi: 10.1186/s11671-026-04507-8.

[28] S. S. Joshi and A. S. Dhoble, "Analytical approach for performance estimation of BSPVT system with liquid spectrum filters," Energy, vol. 157, pp. 778-791, 2018, doi: 10.1016/j.energy.2018.05.204.